

An investigation of transmission control measures during the first 50 days of the COVID-19 epidemic in China

Huaiyu Tian^{1*†}, Yonghong Liu^{1*}, Yidan Li^{1*}, Chieh-Hsi Wu^{3*}, Bin Chen^{4*}, Moritz U.G. Kraemer^{2,5,6}, Bingying Li¹, Jun Cai⁷, Bo Xu⁷, Qiqi Yang¹, Ben Wang¹, Peng Yang⁸, Yujun Cui⁹, Yimeng Song¹⁰, Pai Zheng¹¹, Quanyi Wang⁸, Ottar N. Bjornstad^{12,13}, Ruifu Yang^{8†}, Bryan T. Grenfell^{14,15†}, Oliver G. Pybus^{2†}, Christopher Dye^{2†}

¹ State Key Laboratory of Remote Sensing Science, College of Global Change and Earth System Science, Beijing Normal University, Beijing, China

² Department of Zoology, University of Oxford, Oxford, UK

³ Mathematical Sciences, University of Southampton, Southampton, United Kingdom

⁴ Department of Land, Air and Water Resources, University of California Davis, CA, USA

⁵ Harvard Medical School, Harvard University, Boston, MA, USA

⁶ Boston Children's Hospital, Boston, MA, USA

⁷ Ministry of Education Key Laboratory for Earth System Modeling, Department of Earth System Science, Tsinghua University, Beijing, China

⁸ Beijing Center for Disease Prevention and Control, Beijing, China

⁹ State Key Laboratory of Pathogen and Biosecurity, Beijing Institute of Microbiology and Epidemiology, Beijing, China

¹⁰ Department of Urban Planning and Design, The University of Hong Kong, Hong Kong

¹¹ Department of Occupational and Environmental Health Sciences, School of Public Health, Peking University, China

¹² Center for Infectious Disease Dynamics, Department of Biology, Pennsylvania State University, University Park, Pennsylvania, USA

¹³ Department of Entomology, College of Agricultural Sciences, Pennsylvania State University, University Park, Pennsylvania, USA

¹⁴ Division of International Epidemiology and Population Studies, Fogarty International Center, National Institutes of Health, Bethesda, MD, USA

¹⁵ Department of Ecology and Evolutionary Biology, Princeton University, Princeton, NJ, USA.

*These authors contributed equally to this work.

†Corresponding author. Email: tianhuaiyu@gmail.com (H.T.); christopher.dye@zoo.ox.ac.uk (C.D.); oliver.pybus@zoo.ox.ac.uk (O.G.P.); grenfell@princeton.edu (B.G.); ruifuyang@gmail.com (R.F.Y.);

38 **One sentence summary**

39 China's national emergency response appears to have delayed epidemic growth and limited the
40 number of cases during the first 50 days of the COVID-19 epidemic.

41
42 **Abstract (150 words)**

43 Responding to an outbreak of a novel coronavirus (agent of COVID-19) in December 2019, China
44 banned travel to and from Wuhan city on 23 January and implemented a national emergency
45 response. We investigated the spread and control of COVID-19 using a unique data set including
46 case reports, human movement and public health interventions. The Wuhan shutdown was
47 associated with the delayed arrival of COVID-19 in other cities by 2.91 days (95%CI: 2.54-3.29).
48 Cities that implemented control measures pre-emptively reported fewer cases, on average, in the
49 first week of their outbreaks (13.0; 7.1-18.8) compared with cities that started control later (20.6;
50 14.5-26.8). Suspending intra-city public transport, closing entertainment venues and banning
51 public gatherings were associated with reductions in case incidence. The national emergency
52 response appears to have delayed the growth and limited the size of the COVID-19 epidemic in
53 China, averting hundreds of thousands of cases by 19 February (day 50).

54
55 *Key words:* novel coronavirus, COVID-19, epidemic, emergency, transmission control, Wuhan
56 city, China

Main text

On 31 December 2019, less than a month before the 2020 Spring Festival holiday, including the Chinese Lunar New Year, a cluster of pneumonia cases caused by an unknown pathogen was reported in Wuhan, a city of 11 million inhabitants and the largest transport hub in Central China. A novel coronavirus (*1*, *2*) was identified as the etiological agent (*3*, *4*) and human-to-human transmission of the virus (SARS-CoV-2) has been since confirmed (*5*, *6*). Further spatial spread of this disease was of great concern in view of the upcoming Spring Festival (“*chunyun*”) during which there are typically three billion travel movements over the 40-day holiday period, which runs from 15 days before the Spring Festival (Chinese Lunar New Year) to 25 days afterwards (*7*, *8*).

As there is currently neither a vaccine nor a specific drug treatment for COVID-19, a range of public health (non-pharmaceutical) interventions has been used to control the epidemic. In an attempt to prevent further dispersal of COVID-19 from its source, all transport was prohibited in and out of Wuhan city from 10:00h on 23 January 2020, followed by the whole of Hubei Province a day later. In terms of the population covered, this appears to be the largest attempted cordon sanitaire in human history.

On 23 January, China also raised its national public health response to the highest state of emergency—Level 1 of 4 levels of severity in the Chinese Emergency System, defined as an “extremely serious incident” (*9*). As part of the national emergency response, and in addition to the Wuhan city travel ban, suspected and confirmed cases have been isolated, public transport by bus and subway rail suspended, schools and entertainment venues have been closed, public gatherings banned, health checks carried out on migrants (“floating population”), travel prohibited in and out of cities, and information widely disseminated. Despite all these measures, COVID-19 remains a danger in China. Control measures taken in China potentially hold lessons for other countries around the world.

Although the spatial spread of infectious diseases has been intensively studied (*10-15*), including explicit studies of the role of human movement (*16*, *17*), the effectiveness of travel restrictions and social distancing measures in preventing the spread of infection is uncertain. For COVID-19, coronavirus transmission patterns and the impact of interventions are still poorly understood (*6*, *7*). We therefore carried out a quantitative analysis to investigate the role of travel restrictions and transmission control measures during the first 50 days of the COVID-19 epidemic in China, from 31 December 2019 to 19 February 2020 (Fig. 1). This period encompassed the 40 days of the Spring Festival holiday, 15 days before the Chinese Lunar New Year on 25 January and 25 days afterwards. The analysis is based on a unique geocoded repository of data on COVID-19 epidemiology, human movement, and public health (non-pharmaceutical) interventions. These data include the numbers of COVID-19 cases reported each day in each city of China, information on 4.3 million human movements from Wuhan city, and data on the timing and type of transmission control measures implemented across cities of China.

We first investigated the role of the Wuhan city travel ban, comparing travel in 2020 with that in previous years and exploring how holiday travel links to the dispersal of infection across China.

During Spring Festival travel in 2017 and 2018, there was an average outflow of 5.2 million people from Wuhan city during the 15 days before the Chinese Lunar New Year. In 2020, this travel was interrupted by the Wuhan city shutdown, but 4.3 million people travelled out of the city between 11 January and the implementation of the ban on 23 January (7) (Fig. 2A). In 2017 and 2018, travel out of the city during the 25 days after the Chinese Lunar New Year averaged 6.7 million people each year. In 2020, the travel ban prevented almost all of that movement and markedly reduced the number of exportations of COVID-19 from Wuhan (7, 8).

The dispersal of COVID-19 from Wuhan was rapid (Fig. 3A). A total of 262 cities reported cases within 28 days. For comparison, the 2009 influenza H1N1 pandemic took 132 days to reach the same number of cities in China (see methods in Supplementary Materials). The number of cities providing first reports of COVID-19 peaked at 59 per day on 23 January, the date of the Wuhan travel ban.

The total number of cases reported from each province by 30 January, one week after the Wuhan shutdown, was strongly associated with the total number of travellers from Wuhan ($r=0.98$, $P<0.01$; excluding Hubei, $r=0.69$, $P<0.01$; Figs. 2B and 2C). COVID-19 arrived sooner in those cities that had larger populations and had more travellers from Wuhan (Tables 1 and S1). However, the Wuhan travel ban was associated with a delayed arrival time of COVID-19 in other cities by an estimated 2.91 days (95%CI: 2.54-3.29 days) on average (Table 1, Fig. 3B).

This delay provided extra time to prepare for the arrival of COVID-19 in more than 130 cities across China but would not have curbed transmission after infection had been exported to new locations from Wuhan. Fig. 1 shows the timing and implementation of emergency control measures in 342 cities across China (see also Figs. S2 and S4). School closure, the isolation of suspected and confirmed patients, plus the disclosure of information was implemented in all cities. Public gatherings were banned and entertainment venues closed in 220 cities (64.3%). Intra-city public transport was suspended in 136 cities (39.7%) and inter-city travel was prohibited by 219 cities (64.0%). All three measures were applied in 136 cities (Table S2).

Cities that implemented a Level 1 response (any combination of control measures; Figs. S2 and S4) pre-emptively, before discovering any COVID-19 cases, reported 33.3% (95%CI: 11.1-44.4%) fewer laboratory-confirmed cases during the first week of their outbreaks (13.0, 95%CI: 7.1-18.8, $n=125$) compared with cities that started control later (20.6 cases, 95%CI: 14.5-26.8, $n=171$), with a statistically significant difference between the two groups (Mann-Whitney $U=8197$ $z=-3.4$, $P<0.01$). A separate analysis using regression models shows that, among specific control measures, cities that suspended intra-city public transport and/or closed entertainment venues and banned public gatherings, and did so sooner, had fewer cases during the first week of their outbreaks (Table 2, Table S3). This analysis provided no evidence that the prohibition of travel between cities, which was implemented after and in addition to the Wuhan shutdown on 23 January, reduced the number of cases in other cities across China. These results are robust to the choice of statistical regression model (Table S3).

The reported daily incidence of confirmed cases peaked in Hubei province (including Wuhan) on

145 4 February (3156 laboratory-confirmed cases, 5.33/100,000 population in Hubei), and in all other
 146 provinces on 31 January (875 cases, 0.07/100,000 population; Fig. S1). The low level of peak
 147 incidence per capita, the early timing of the peak, and the subsequent decline in daily case reports,
 148 suggest that transmission control measures were not only associated with a delay in the growth of
 149 the epidemic, but also with a marked reduction in the number of cases. By fitting an epidemic
 150 model to the time series of cases reported in each province (Fig. S3), we estimate that the (basic)
 151 case reproduction number (R_0) was 3.15 prior to the implementation of the emergency response on
 152 23 January (Table 3). As control was scaled-up from 23 January onwards (stage 1), the case
 153 reproduction number declined to 0.97, 2.01 and 3.05 (estimated as C_1R_0) in three groups of
 154 provinces, depending on the rate of implementation in each group (Tables 3 and S4). Once the
 155 implementation of interventions was 95% complete everywhere (stage 2), the case reproduction
 156 number had fallen to 0.04 on average (C_2R_0), far below the replacement rate ($\ll 1$) and consistent
 157 with the rapid decline in incidence (Fig. 4A, Fig. S5, Table 3, Table S4).

158
 159 Based on the fit of the model to daily case reports from each province, and on the preceding
 160 statistical analyses, we investigated the possible effects of control measures on the trajectory of the
 161 epidemic outside Wuhan city (Fig. 4B). Our model suggests that, without the Wuhan travel ban or
 162 the national emergency response, there would have been 744,000 ($\pm 156,000$) confirmed
 163 COVID-19 cases outside Wuhan by 19 February, day 50 of the epidemic. With the Wuhan travel
 164 ban alone, this number would have decreased to 202,000 ($\pm 10,000$) cases. With the national
 165 emergency response alone (without the Wuhan travel ban), the number of cases would have
 166 decreased to 199,000 (± 8500). Thus, neither of these interventions would, on their own, have
 167 reversed the rise in incidence by 19 February (Fig. 4B). But together and interactively, these
 168 control measures offer an explanation of why the rise in incidence was halted and reversed,
 169 limiting the number of confirmed cases reported to 29,839 (fitted model estimate $28,000 \pm 1400$
 170 cases), 96% fewer than expected in the absence of interventions.

171
 172 In summary, this analysis shows that transmission control (non-pharmaceutical) measures initiated
 173 during Chinese Spring Festival holiday, including the unprecedented Wuhan city travel ban and
 174 the Level 1 national emergency response, were strongly associated with, though not necessarily
 175 the cause of, a delay in epidemic growth and a reduction in case numbers during the first 50 days
 176 of the COVID-19 epidemic in China.

177
 178 The number of people who have developed COVID-19 during this epidemic, and therefore the
 179 number of people who were protected by control measures, is not known precisely, given that
 180 cases were almost certainly under-reported. However, in view of the small fraction of people
 181 known to have been infected by 19 February (75,532 cases, 5.41 per 100,000 population), it is
 182 unlikely that the spread of infection was halted and epidemic growth reversed because the supply
 183 of susceptible people had been exhausted. This implies that a large fraction of the Chinese
 184 population remains at risk of COVID-19; control measures may need to be reinstated, in some
 185 form, if there is a resurgence of transmission. Further investigations are needed to verify that
 186 proposition, and population surveys of infection are needed to reveal the true number of people
 187 who have been exposed to this novel coronavirus.

188

We could not investigate the impact of all elements of the national emergency response because many were introduced simultaneously across China. However, this analysis shows that suspending intra-city public transport, closing entertainment venues and banning public gatherings, which were introduced at different times in different places, were associated with the overall containment of the epidemic. However, other factors are likely to have contributed to control, especially the isolation of suspected and confirmed patients and their contact, and it is not yet clear which parts of the national emergency response were most effective. We did not find evidence for prohibiting travel between cities or provinces reduced the numbers of COVID-19 cases outside Wuhan and Hubei, perhaps because such travel bans were implemented as a response to, rather than in anticipation of, the arrival of COVID-19.

This study has drawn inferences, not from controlled experiments, but from statistical and mathematical analyses of the temporal and spatial variation in case reports, human mobility and transmission control measures. With that caveat, control measures were strongly associated with the containment of COVID-19, potentially averting hundreds of thousands of cases by 19 February, day 50 of the epidemic. Whether the means and the outcomes of control can be replicated outside China, and which of the interventions are most effective, are now under intense investigation as the virus continues to spread worldwide.

References and Notes

1. N. Zhu, D. Zhang, W. Wang, X. Li, B. Yang, J. Song, X. Zhao, B. Huang, W. Shi, R. Lu, P. Niu, F. Zhan, X. Ma, D. Wang, W. Xu, G. Wu, G. F. Gao, W. Tan, A novel coronavirus from patients with pneumonia in China, 2019. *New Eng J Med* **382**, 727-733 (2020).
2. R. Lu, X. Zhao, J. Li, P. Niu, B. Yang, H. Wu, W. Wang, H. Song, B. Huang, N. Zhu, Genomic characterisation and epidemiology of 2019 novel coronavirus: implications for virus origins and receptor binding. *Lancet* **395**, 565-574 (2020).
3. F. Wu, S. Zhao, B. Yu, Y.-M. Chen, W. Wang, Z.-G. Song, Y. Hu, Z.-W. Tao, J.-H. Tian, Y.-Y. Pei, M.-L. Yuan, Y.-L. Zhang, F.-H. Dai, Y. Liu, Q.-M. Wang, J.-J. Zheng, L. Xu, E. C. Holmes, Y.-Z. Zhang, A new coronavirus associated with human respiratory disease in China. *Nature* **579**, 265-269 (2020).
4. P. Zhou, X.-L. Yang, X.-G. Wang, B. Hu, L. Zhang, W. Zhang, H.-R. Si, Y. Zhu, B. Li, C.-L. Huang, H.-D. Chen, J. Chen, Y. Luo, H. Guo, R.-D. Jiang, M.-Q. Liu, Y. Chen, X.-R. Shen, X. Wang, X.-S. Zheng, K. Zhao, Q.-J. Chen, F. Deng, L.-L. Liu, B. Yan, F.-X. Zhan, Y.-Y. Wang, G.-F. Xiao, Z.-L. Shi, A pneumonia outbreak associated with a new coronavirus of probable bat origin. *Nature* **579**, 270-273 (2020).
5. J. Cai, B. Xu, K. K. Y. Chan, X. Zhang, B. Zhang, Z. Chen, B. Xu, Roles of Different Transport Modes in the Spatial Spread of the 2009 Influenza A (H1N1) Pandemic in Mainland China. *Int J Environ Res Public Health* **16**, 222 (2019).
6. C. Wang, P. W. Horby, F. G. Hayden, G. F. Gao, A novel coronavirus outbreak of global health concern. *Lancet* **395**, 470-473 (2020).
7. C. Simiao, Y. Juntao, Y. Weizhong, W. Chen, B. Till, COVID-19 control in China during mass population movements at New Year. *Lancet* **395**, 764-766 (2020).
8. M. U. G. Kraemer, C.-H. Yang, B. Gutierrez, C.-H. Wu, B. Klein, D. M. Pigott, L. du Plessis, N. R. Faria, R. Li, W. P. Hanage, J. S. Brownstein, M. Layan, A. Vespignani, H. Tian, C. Dye,

- 233 O. G. Pybus, S. V. Scarpino, The effect of human mobility and control measures on the
234 COVID-19 epidemic in China. *Science*, eabb4218 (2020)10.1126/science.abb4218).
- 235 9. Chinadaily, "Tibet activates highest-level public health alert" (Jan 30, 2020).
236 <https://www.chinadaily.com.cn/a/202001/202029/WS202005e202318a202036a3101282172739c3101282172731.html>.
237
- 238 10. B. T. Grenfell, O. N. Bjørnstad, J. Kappey, Travelling waves and spatial hierarchies in
239 measles epidemics. *Nature* **414**, 716-723 (2001).
- 240 11. D. Brockmann, D. Helbing, The hidden geometry of complex, network-driven contagion
241 phenomena. *Science* **342**, 1337-1342 (2013).
- 242 12. A. Wesolowski, N. Eagle, A. J. Tatem, D. L. Smith, A. M. Noor, R. W. Snow, C. O. Buckee,
243 Quantifying the impact of human mobility on malaria. *Science* **338**, 267-270 (2012).
- 244 13. N. M. Ferguson, D. A. Cummings, S. Cauchemez, C. Fraser, S. Riley, A. Meeyai, S.
245 Iamsirithaworn, D. S. Burke, Strategies for containing an emerging influenza pandemic in
246 Southeast Asia. *Nature* **437**, 209-214 (2005).
- 247 14. K. E. Jones, N. G. Patel, M. A. Levy, A. Storeygard, D. Balk, J. L. Gittleman, P. Daszak, Global
248 trends in emerging infectious diseases. *Nature* **451**, 990-993 (2008).
- 249 15. D. M. Morens, G. K. Folkers, A. S. Fauci, The challenge of emerging and re-emerging
250 infectious diseases. *Nature* **430**, 242-249 (2004).
- 251 16. C. Viboud, O. N. Bjørnstad, D. L. Smith, L. Simonsen, M. A. Miller, B. T. Grenfell, Synchrony,
252 waves, and spatial hierarchies in the spread of influenza. *Science* **312**, 447-451 (2006).
- 253 17. A. Wesolowski, T. Qureshi, M. F. Boni, P. R. Sundsøy, M. A. Johansson, S. B. Rasheed, K.
254 Engø-Monsen, C. O. Buckee, Impact of human mobility on the emergence of dengue
255 epidemics in Pakistan. *Proc Natl Acad Sci USA* **112**, 11887-11892 (2015).
- 256 18. H. Tian, Y. Liu, Y. Li, C.-H. Wu, B. Chen, M. U. Kraemer, B. Li, J. Cai, B. Xu, Q. Yang, B. Wang,
257 P. Yang, Y. Cui, Y. Song, P. Zheng, Q. Wang, O. N. Bjørnstad, R. Yang, B. T. Grenfell, O. G.
258 Pybus, C. Dye, Code for: An investigation of transmission control measures during the
259 first 50 days of the COVID-19 epidemic in China. *Zenodo*,
260 <https://doi.org/10.5281/zenodo.3727336> (2020).
- 261 19. J. T. Wu, K. Leung, G. M. Leung, Nowcasting and forecasting the potential domestic and
262 international spread of the 2019-nCoV outbreak originating in Wuhan, China: a
263 modelling study. *Lancet* **395**, 689-697 (2020).
- 264 20. B. Ripley, B. Venables, D. M. Bates, K. Hornik, A. Gebhardt, D. Firth, M. B. Ripley, Package
265 'MASS'. *CRAN Repository*, See <http://cran.r-project.org/web/packages/MASS/MASS.pdf>
266 (2013).
- 267 21. B. R. Kirkwood, J. A. Sterne, *Essential medical statistics*. (John Wiley & Sons, 2010).
- 268 22. D. E. Bailey, *Probability and Statistics*. (John Wiley & Sons, 1971).
- 269 23. A. Canty, B. Ripley, boot: Bootstrap R (S-Plus) functions. R package version 1.3-24.
270 (2019).
- 271 24. A. C. Davison, D. V. Hinkley, *Bootstrap methods and their application*. (Cambridge
272 university press, Cambridge, 1997).
- 273 25. R. M. Anderson, R. M. May, *Infectious Diseases of Humans: Dynamics and Control*.
274 (Oxford Univ Press, Oxford, 1992).
- 275 26. A. Morton, B. F. Finkenstädt, Discrete time modelling of disease incidence time series by
276 using Markov chain Monte Carlo methods. *J R Stat Soc C* **54**, 575-594 (2005).

- 277 27. Q. Li, X. Guan, P. Wu, X. Wang, L. Zhou, Y. Tong, R. Ren, K. S. M. Leung, E. H. Y. Lau, J. Y.
 278 Wong, X. Xing, N. Xiang, Y. Wu, C. Li, Q. Chen, D. Li, T. Liu, J. Zhao, M. Li, W. Tu, C. Chen, L.
 279 Jin, R. Yang, Q. Wang, S. Zhou, R. Wang, H. Liu, Y. Luo, Y. Liu, G. Shao, H. Li, Z. Tao, Y.
 280 Yang, Z. Deng, B. Liu, Z. Ma, Y. Zhang, G. Shi, T. T. Y. Lam, J. T. K. Wu, G. F. Gao, B. J.
 281 Cowling, B. Yang, G. M. Leung, Z. Feng, Early transmission dynamics in Wuhan, China, of
 282 novel coronavirus-infected pneumonia. *N Engl J Med* **382**, 1199-1207
 283 (2020)10.1056/NEJMoa2001316).
- 284 28. O. N. Bjørnstad, R. A. Ims, X. Lambin, Spatial population dynamics: analyzing patterns and
 285 processes of population synchrony. *Trends Ecol Evol* **14**, 427-432 (1999).

286

287 **Acknowledgements**

288 We thank the thousands of CDC staff and local health workers in China who collected data and
 289 continue to work to contain COVID-19 in China and elsewhere. **Funding:** this study was provided
 290 by the National Natural Science Foundation of China (81673234); Beijing Natural Science
 291 Foundation (JQ18025); Beijing Advanced Innovation Program for Land Surface Science; Young
 292 Elite Scientist Sponsorship Program by CAST (YESS)(2018QNRC001); HT, MUGK, OGP and
 293 CD acknowledge support from the Oxford Martin School; HT acknowledges support from the
 294 Military Logistics Research Program. The funders had no role in study design, data collection and
 295 analysis, the decision to publish, or in preparation of the manuscript. **Author contributions:** H.T.,
 296 P.Z., R.F.Y., O.G.P., B.T.G., C.D. designed the study. B.C. and Y.M.S. collected and processed the
 297 Tencent's LBS data. Y.H.L., B.Y.L., B.X., Q.Q.Y., B.W., P.Y., Y.J.C., Q.Y.W. collected the
 298 statistical data. H.Y.T., Y.L., C.H.W. and J.C. conducted the analyses. M.K., O.N.B., R.F.Y., O.G.P.,
 299 B.T.G., and C.D. edited the manuscript. H.T. and C.D. wrote the manuscript. All authors read and
 300 approved the manuscript. **Competing interests:** All other authors declare no competing interests.
 301 **Data and materials availability:** Code and data are available on the following GitHub repository:
 302 https://github.com/huaiyutian/COVID-19_TCM-50d_China here (18).

303

304 **Supplementary Materials**

305 **Materials and Methods**

306 Fig S1 – S7

307 Table S1 – S4

308 References 19 – 28

309

310

311

312 **Table 1.** Association between the Wuhan travel ban and COVID-19 dispersal to other cities in
 313 China.

314

Covariates	Coefficient	95% CI	P
Intercept	25.95	(23.43, 28.48)	<0.01
Longitude (degrees)	-0.03	(-0.05, -0.01)	<0.01
Latitude (degrees)	0.03	(0.01, 0.06)	<0.05
log10 (population)	-0.70	(-1.12, -0.28)	<0.01
log10 (total movements)	-0.12	(-0.22, -0.02)	<0.05
Travel ban (days)	2.91	(2.54, 3.29)	<0.01

315

The dependent variable Y is the arrival time (days) of the outbreak in each city

316

317

318

319

320

321

322

323

324

325

326

327

328 **Table 2.** Associations between the type and timing of transmission control measures and the
 329 number of COVID-19 cases reported in city outbreaks (first week), evaluated by a generalised
 330 linear regression model.

331

Covariates	Coefficient	95% CI	P*
(Intercept)	-9.10	(-9.56, -8.64)	<0.01
Arrival time	0.44	(0.43, 0.46)	<0.01
Distance from Wuhan City (log10)	0.61	(0.49, 0.73)	<0.01
Suspension of intra-city public transport			
Implementation	-3.50	(-4.28, -2.73)	<0.01
Timing	0.11	(0.08, 0.14)	<0.01
Closure of entertainment venues			
Implementation	-2.28	(-2.98, -1.57)	<0.01
Timing	0.09	(0.06, 0.11)	<0.01

332

333

334

335

336

337

338

339

340

341

342

343

344 **Table 3.** Parameter estimates of the SEIR epidemic model.

345

Parameter	Definition	Mean	95%BCI
ρ	Reporting rate (proportion)	0.002	0.001-0.003
R_0	Basic reproduction number	3.15	3.04-3.26
$1/\delta$	Mean incubation period (days)	4.90	4.32-5.47
C_{1_high}	Lower effect of control at the first stage	0.97	0.94-0.99
C_{1_medium}	Medium effect of control at the first stage	0.65	0.58-0.72
C_{1_low}	Higher effect of control at the first stage	0.31	0.24-0.38
C_2	Effect of control at the second stage	0.01	0.001-0.03
$1/\gamma$	Infectious period before isolation (days)	5.19	4.51-5.86
I_{w0}	Minimum number of cases when none detected	1.12	0.91-1.32

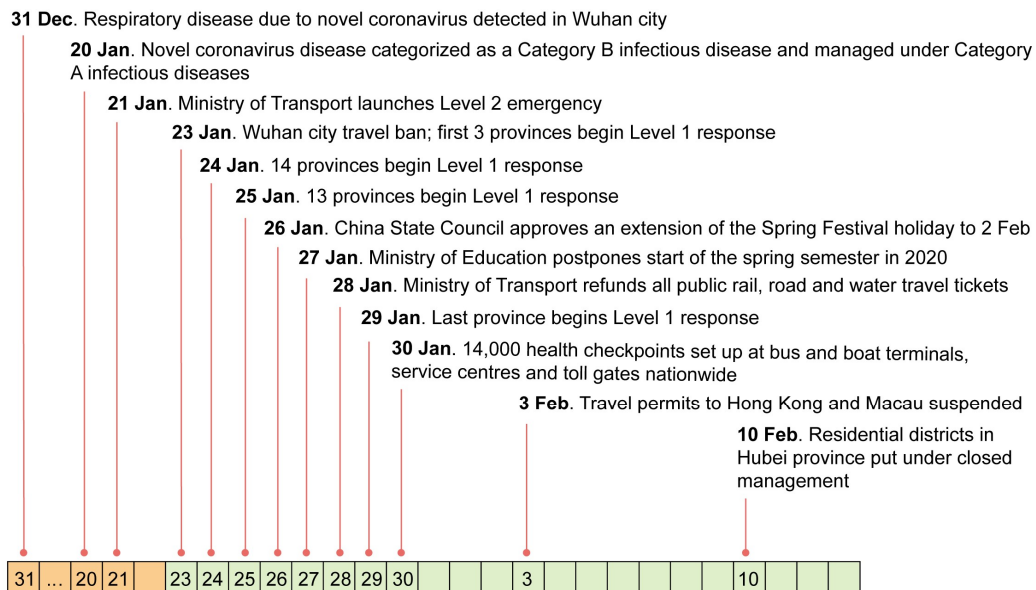
346 BCI: Bayesian confidence interval

347 C_{1_high} : Heilongjiang, Shanghai, Tianjin, Zhejiang, Hubei (exclude Wuhan)348 C_{1_medium} : Anhui, Beijing, Fujian, Guangdong, Guangxi, Guizhou, Hunan, Jilin, Jiangsu, Jiangxi,
349 Inner Mongolia, Shandong, Tibet350 C_{1_low} : Gansu, Hainan, Hebei, Henan, Liaoning, Ningxia, Qinghai, Shanxi, Shaanxi, Sichuan,
351 Xinjiang, Yunnan, Chongqing

352

353

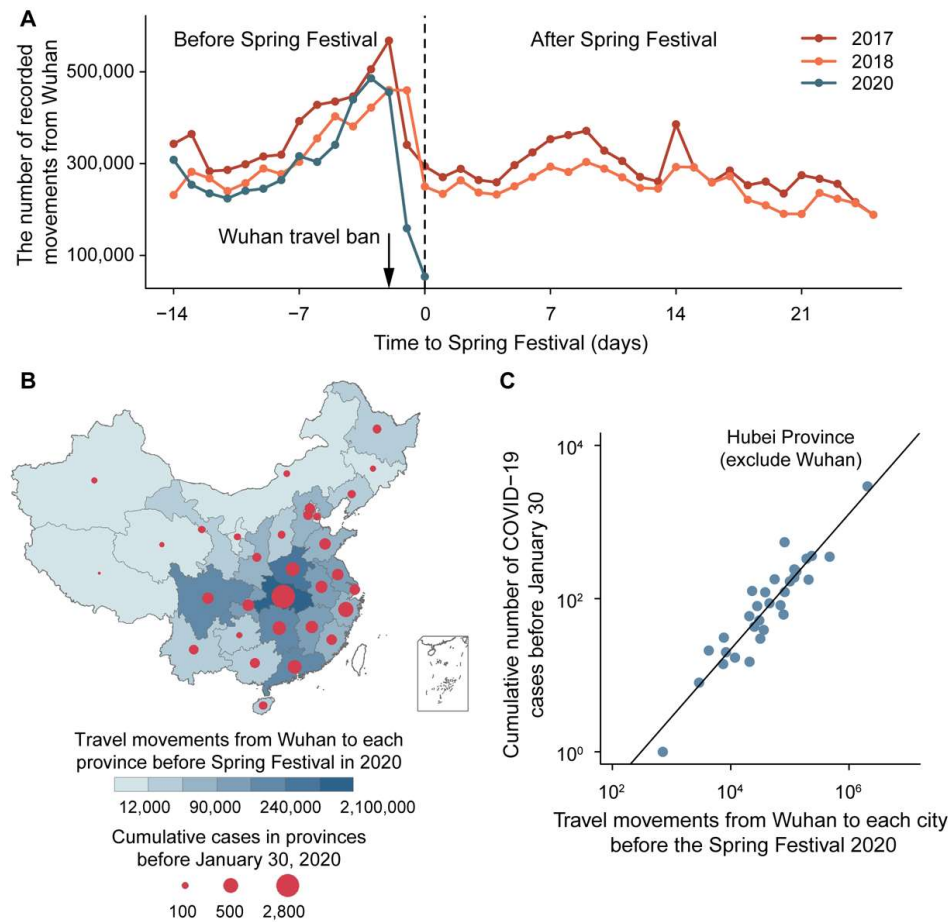
354
355



356
357
358
359
360

Figure 1. Dates of discovery of the novel coronavirus causing COVID-19, and of the implementation of control measures in China, from 31 December 2019.

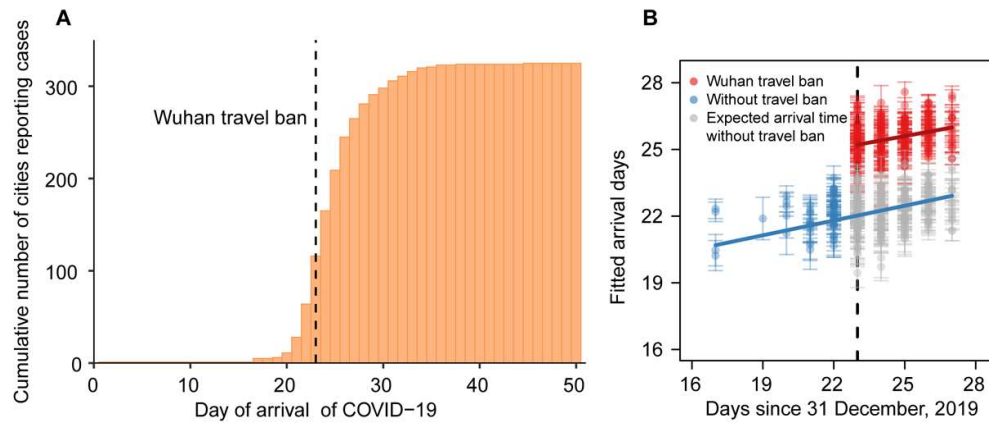
361
362



363
364
365
366
367
368
369
370
371
372
373
374
375

Figure 2. The dispersal of COVID-19 in China 15 days before and 25 days after the Spring Festival (Chinese Lunar New Year). (A) Movement outflows from Wuhan City during Spring Festival travel in 2017, 2018, and 2020. The vertical dotted line is the date of Spring Festival (Chinese Lunar New Year). (B) The number of recorded movements from Wuhan city to other provinces during the 15 days before the Spring Festival in 2020. The shading from light to dark represents the number of human movements from Wuhan to each province. The area of circles represents the cumulative number of cases reported by 30 January 2020, one week after the Wuhan travel ban on 23 January. (C) Association between the cumulative number of confirmed cases reported before 30 January and the number of movements from Wuhan to other provinces.

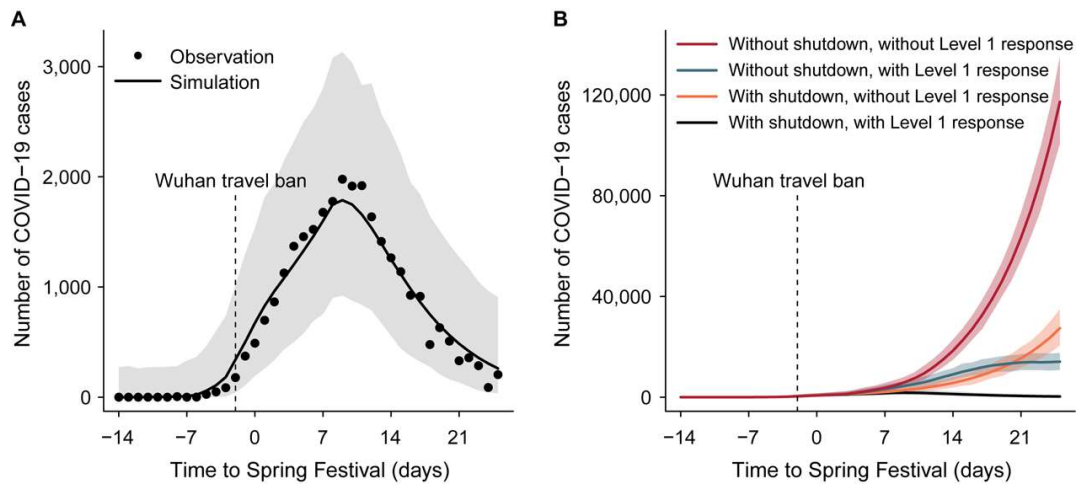
376
377



378
379
380
381
382
383
384
385
386
387
388
389
390
391

Figure 3. Spatial dispersal of COVID-19 in China. (A) Cumulative number of cities reporting cases by 19 February 2020. Arrival days, defined as the time interval (days) from the date of the first case in the first infected city (Wuhan) to the date of the first case in each newly infected city (a total of 324 cities), to characterize the inter-city transmission rate of COVID-19. Dashed line shows the date of Wuhan travel ban (shutdown). (B) Before (blue) and after (red) the intervention by 30 January 2020, one week after Wuhan travel ban (shutdown). The blue line and points show the fitted regression of arrival times up to the shutdown on day 23 (23 January, vertical dashed line). Grey points show the expected arrival times after day 23, without the shutdown. The red line and points show the fitted regression of delayed arrival times after the shutdown on day 23. Each observation (point) represents one city. Error bars give ± 2 standard deviations.

392
393



394
395
396
397
398
399
400
401
402
403
404

Figure 4. The role of interventions in controlling the COVID-19 outbreak across China. (A) Epidemic model (line) fitted to daily reports of confirmed cases (points) summed across 31 provinces. Hubei excludes Wuhan city. (B) Expected epidemic trajectories without the Wuhan travel ban (shutdown), and with (green) or without (red) interventions carried out as part of the Level 1 national emergency response; with the Wuhan travel ban, and with (black) or without the intervention (orange). Vertical dashed lines in both panels mark the date of the Wuhan travel ban and the start of the emergency response, on 23 January. Shaded regions in A and B mark the 95% prediction envelopes.



Supplementary Materials for

An investigation of transmission control measures during the first 50 days
of the COVID-19 epidemic in China

Huaiyu Tian, Yonghong Liu, Yidan Li, Chieh-Hsi Wu, Bin Chen, Moritz U.G.
Kraemer, Bingying Li, Jun Cai, Bo Xu, Qiqi Yang, Ben Wang, Peng Yang, Yujun Cui,
Yimeng Song, Pai Zheng, Quanyi Wang, Ottar N. Bjornstad, Ruifu Yang, Bryan T.
Grenfell, Oliver G. Pybus, Christopher Dye

Correspondence to: tianhuaiyu@gmail.com; christopher.dye@zoo.ox.ac.uk;
oliver.pybus@zoo.ox.ac.uk; grenfell@princeton.edu; ruifuyang@gmail.com;

This PDF file includes:

Materials and Methods
Figs. S1 to S7
Tables S1 to S4
References

Materials and Methods

Epidemiological, demographic and geographical data

We collected data from the official reports of the health commission of 34 provincial-level administrative units and 342 city-level units. We recorded the date of the first reported case in all newly-infected cities, including daily reports from 31 December 2019 to 19 February 2020, the first 50 days of the epidemic. Only laboratory-confirmed cases of COVID-19 were used. Population sizes for each city in 2018 were obtained from the China City Statistical Yearbook (<http://olap.epsnet.com.cn/>). Using ArcGIS we calculated the great circle distance between Wuhan and each city reporting COVID-19 cases. The location of each city is geocoded by the latitude and longitude coordinates of the city centre. To make a comparison with the 2009 H1N1 Pandemic (2009-H1N1pdm), daily case data were collected from China Information System for Disease Control and Prevention (CISDCP) from 10 May 2009 to 30 April 2010, a total of more than 180,000 cases (5).

Human mobility data

Human movements were tracked with mobile phone data, through location-based services (LBS) employed by popular Tencent applications such as WeChat and QQ. Movement outflows from Wuhan City to other cities (i.e. records of the number of people leaving each day) by air, train and road, were obtained from the migration flows database (<https://heat.qq.com/>) (19) from 13 January 2017 to 21 February 2017 (Spring Festival travel 2017), from 1 February 2018 to 12 March 2018 (Spring Festival travel 2018), and from 1 January 2018 to 31 December 2018 (entire 2018). To reconstruct the movement outflow from Wuhan during the 2020 Spring Festival (from 11 January to 25 January, before the Chinese Lunar New Year), mobile phone data (provided by the telecommunications operators) were used together with the Baidu migration index (<http://qianxi.baidu.com/>); using both data sources gave the most accurate measure of movement volume. The expected movement outflows from Wuhan after the New Year festival from 26 January to 19 February, had there been no travel ban, were generated by using travel volumes for 2017 and 2018 and the recorded travel destinations prior to the shutdown in 2020. We assumed that the proportion of daily outflows from Wuhan to each of the other destinations in China was constant through time.

Association between the Wuhan city travel ban and the arrival time of COVID-19 in other cities

In order to quantify the association between the Wuhan travel shutdown (23 January 2020) and COVID-19 spread, we used data collected between 31 December 2019 and 28 January 2020. The association between distance, human movement, interventions and timing of COVID-19 spread was assessed by a linear regression. Among five possible regression models examined (Table S3), the model judged best by the Akaike Information Criterion) was:

$$E[Y_i] = \alpha + \beta_1 \log_{10}(TotalFlow_i) + \beta_2 \log_{10}(Pop_i) + \beta_3 Long_i + \beta_4 Lat_i + \beta_5 Shutdown_i$$

Dependent variable Y_i is the arrival time (day) of the first confirmed case in city i , a measure of the spatial spread of COVID-19. The β_j 's are the regression coefficients. α is the intercept. $TotalFlow_i$ represents the passenger volume from Wuhan to city i by airplane, train and road during the whole of 2018. Pop_i is the population of city i . Lat_i and $Long_i$ represent the latitude and longitude of city

479 *i*. The binary dummy variable *Shutdown_i* is used to identify whether the arrival time of COVID-19
480 in newly-infected city *i* is associated with the Wuhan travel ban. For each city, *Shutdown* was set
481 to 0 for arrival before 23 January 2020 and 1 for arrival on or after 23 January 2020. The
482 regression analysis was performed using the R version 3.4.0. All of the candidate models
483 examined (Table S3) produced similar estimates for the estimated delay in the arrival time due to
484 the shutdown.

485

486 Diagnostic analyses were performed to check whether model assumptions have been violated.
487 “Residuals” in this section refers to the residuals of linear regression model for travel ban. Spatial
488 coordinates (*Lat* and *Long*) and passenger volume from Wuhan (*TotalFlow*) were included to adjust
489 for possible spatial and temporal autocorrelation, respectively. However, we performed additional
490 checks to investigate whether there was spatial autocorrelation among the residuals, which could
491 contribute to data dependency.

492

493 If there were spatial autocorrelation in the residuals, then the pairwise residual differences of cities
494 closer together would tend to be smaller than those of cities far apart. In other words, we would
495 expect a high correlation between the pairwise differences in residuals and pairwise distances of
496 cities. Such a correlation was not evident ($r=0.03$).

497

498 Differential accessibility from Wuhan to other cities may contribute to data-dependence. Therefore,
499 we examined the timing of peak inflow from Wuhan City and the arrival time of COVID-19 in
500 each city. The result shows no evident correlation between them ($r=-0.07$, $P=0.25$). In addition, we
501 calculated the correlation between the residuals and peak time of Wuhan inflow during 11 to 23
502 January (15 days before Chinese New Year to the Wuhan shutdown). Again, we found no evident
503 correlation ($r=0.08$).

504

505 We did not detect issues regarding heteroscedasticity (studentized Breuch-Pagan test $P=0.20$) nor
506 normality (Shapiro-Wilk test $P=0.06$). The residuals generally lie close to the straight line in the
507 Q-Q plot (Fig. S6). Therefore, it is not evident that the distribution of errors departs from a normal
508 distribution.

509

510 The associations between transmission control measures and the number of cases reported during
511 the first week of an outbreak in a new location

512 The Level 1 national emergency response required suspected and confirmed cases of COVID-19
513 to be isolated and reported immediately in all cities. Using data for 296 cities across China, we
514 investigated the associations between the epidemic intensity and three transmission control
515 measures: closure of entertainment venues and banning public gatherings (*B*); suspension of
516 intra-city public transport (*S*); and prohibition of travel by any means to and from other cities (*P*).
517 The timing of implementation was recorded for each control measure in each city, including the
518 delay in implementation since 31 December 2019 (day 0 of the epidemic). Each city was regarded
519 as implementing an intervention when the official policy was announced publicly (Table S1).
520 Other transmission control measures included delineating control areas, closure of schools,
521 isolation of suspected and confirmed cases, and the disclosure of information. We could not
522 investigate the associations between these interventions and development of the epidemic because

they were reportedly applied in all cities uniformly and without delay.

We perform an association analysis using Poisson regression to investigate how the interventions B , S and P were associated with the dependent (Poisson) variable Y_i —the total number of confirmed cases that were reported during the first seven days of the outbreak in city i . The analysis was performed by using the GLM function in the MASS package (20) in R (version 3.6.2) to construct the model:

$$\log(E[Y_i]) = \alpha + \beta_1 M_{i,S} + \beta_2 M_{i,P} + \beta_3 M_{i,B} + \beta_4 T_{i,S} + \beta_5 T_{i,P} + \beta_6 T_{i,B} + \beta_7 A_i + \beta_8 D_i + \log(Q_i) + \log(F_i),$$

where population size (in millions) (Q_i) and inflow (in millions) from Wuhan (F_i) of city i are offset variables, while the distance to Wuhan (D_i) and the arrival time (A_i) of the infection are adjustments to control for confounding with other independent variables. The β_j 's are regression coefficients. $M_{i,k}$ is a binary variable indicating whether or not control measure k is implemented in city i by the seventh day of the outbreak in that city. $M_{i,k} = 1$, if city i has implemented k before or during its first seven days of outbreak. $M_{i,k} = 0$, if city i has implemented k after its first seven days of outbreak or never implemented k . $T_{i,k}$ represents the timing of implementing control measure k in city i , where 31 December 2019 is day 0. For example, if city i implements control measure k on 27 January 2020, then $T_{i,k} = 27$. If $M_{i,k} = 0$, then $T_{i,k} = 0$. This set up enables the β coefficient of $T_{i,k}$ to only measure the association between Y and the timing variable of k when $M_{i,k} = 1$. D_i is the distance from city i to Wuhan City. A_i is the arrival time of the epidemic in city i (the date of the first confirmed case), where 31 December 2019 is day 0, and for example, if the date of the first confirmed case in city i is on 28 January 2020, then $A_i = 28$.

We detected heteroscedasticity in the Pearson residuals of the Poisson regression model. In attempt to remedy this we applied negative-binomial regression and quasi-poisson regression. Neither methods resolved the issue with heteroscedasticity. Therefore, we resorted to regression models that does not have dependent variables as counts.

To check and confirm the validity of results obtained with the Poisson regression model, we repeated the analysis with a log-linear model. The first step was to standardize case counts by dividing by the number of people in each city (incidence per capita) and the number of people arriving from Wuhan, giving dependent variable Y^* . The log-linear model is then:

$$E[\log(Y_i^*)] = \alpha + \beta_1 M_{i,S} + \beta_3 M_{i,B} + \beta_4 T_{i,S} + \beta_6 C_{i,B} + \beta_7 A_i.$$

The subscripts of the coefficients (β_j) are consistent with a Poisson regression model. We found that the relationship between Y^* and the timing of B is nonlinear. To correct for this, we discretize the timing variable $T_{i,B}$ to obtain an ordinal variable $C_{i,B}$ with four categories, namely 1) 30 December 2019–22 January 2020, 2) 23 January 2020, 3) 24 January 2020 and 4) 25 January onwards. To preserve statistical power, proportional change of $E[Y^*]$ was assumed when moving onto a later category. For example, the difference in $E[\log(Y_i^*)]$ time categories 1 and 2 was assumed the same as that between time categories 2 and 3.

To avoid heteroscedasticity, variables describing the distance from Wuhan, and the implementation and timing of P (prohibiting inter-city travel) were removed. Further exploration of the model showed that these variables did not help to explain the variation in Y^* . Table S3 presents the results of the log-linear regression analysis, which uphold the conclusions reached from the Poisson regression model.

As the purpose of the log-linear regression analysis is to validate the results from the Poisson regression analysis, we performed various diagnostic checks on the log-linear regression model. In summary, we did not find any issues that might invalidate the results. The details of the diagnostic analysis are presented below. “Residuals” in this section refers of the residuals of the log-linear regression model.

As with the regression analysis on the Wuhan city travel ban, we explored whether there is any spatial autocorrelation in the residuals. There was no evident correlation between the pairwise differences in residuals and those of cities ($r=-0.09$). We also examined whether the timing of Wuhan inflow induced dependence in the data. To this end, we evaluated the correlation between the residuals and peak time of inflow from Wuhan to each city during the period from 11 to 23 January. Such correlation is not evident ($r=-0.04$),

In terms of temporal correlation within the residuals, there was no evidence that the mean residuals with arrival time on day j associated with the residuals with arrival time on day $j+1$ ($P=0.80$).

We found no evidence of heteroscedasticity in the residuals (studentised Breusch-Pagan test $P=0.148$). The Shapiro-Wilk test provides evidence against residual normality ($P<0.01$). However, in a sufficiently large dataset such as this one, the Shapiro-Wilk test is very sensitive to departure from normality but does not indicate the severity level of the departure. The Q-Q plot (Fig. S7) indicates a moderate departure from the normal distribution in the residuals, where the histogram indicates that there is a longer right tail (Fig. S7). As the distribution is not severely asymmetric, and our sample size is sufficiently large, this should not be an issue by the central limit theorem (21, 22).

Nevertheless, to ensure the robustness of the conclusions, we also evaluated bootstrap estimates of the regression coefficients, confidence interval and P -value (Table S3) using the R package boot (23, 24). The bootstrap estimates are very similar to the least squared estimates from log-linear regression model (data not shown).

Epidemic modelling

For each province, we estimated the effect of transmission control measures by fitting an SEIR model (25) to the number of new confirmed cases reported each day from each province using Bayesian Markov Chain Monte Carlo methods (26). The model is:

$$\frac{dS_i}{dt} = -I_i \frac{\beta C_{Segment} S_i}{N_i}$$

$$\frac{dE_i}{dt} = I_i \frac{\beta C_{segment} S_i}{N_i} - \delta E_i + \lambda_i$$

$$\frac{dI_i}{dt} = \delta E_i - \gamma I_i$$

$$\frac{dR_i}{dt} = \gamma I_i$$

where S , E , I , and R are the number of susceptible, exposed (latent), infectious, and removed individuals on day t in province i . This standard SEIR model makes some simplifying assumptions: for example, the human population is homogeneous (e.g. not stratified by age or sex), contacts between infectious and susceptible people are also homogeneous (e.g. not stratified by social group) and infection is fully immunizing (I). The model and its assumptions apply only to the first 50 days of the epidemic, the scope of the analysis in this study.

Even with these assumptions, the model describes the data quite accurately for the whole country (Fig. 4A), and reasonably well for each province, with the notable exceptions of Beijing and Shanghai, which had relatively few cases among their well-connected populations (Fig. 4A, Fig. S3). The accuracy of the model's description of national data is remarkably good, given that the model fitting was done separately for each province, and then aggregated to obtain the national total.

The basic reproductive number of the model is $R_0 = \beta/\gamma$, where β is the per capita transmission rate per day and $1/\delta$ and $1/\gamma$ are, respectively, the mean latent and infectious periods.

Variable λ is the estimated number of cases imported from Wuhan City on day t :

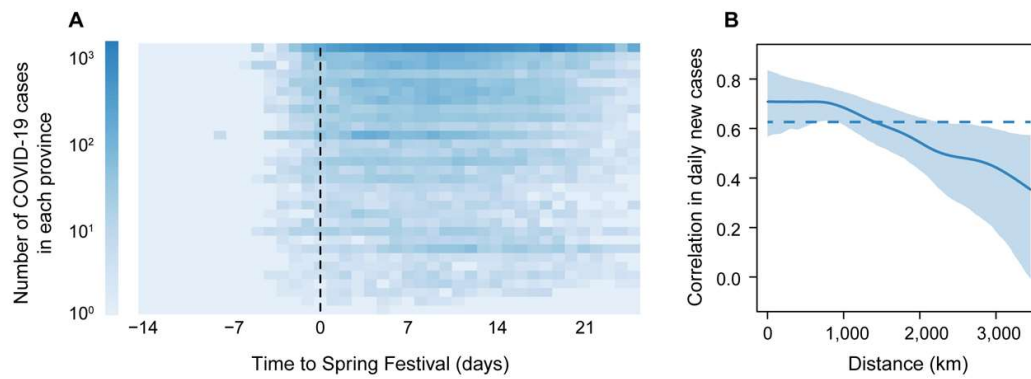
$$\lambda_i(t) = \frac{I_w}{\rho_w P_w} T_i shutdown_w$$

I_w is the number of reported cases in Wuhan on day t , P_w is the Wuhan population size, and ρ_w is the proportion of all infected people (including infectious cases) reported in Wuhan. T_i is the number of people leaving Wuhan on day t travelling to province i , derived from data describing mobility 15 days before the Chinese Lunar New Year 2020. The binary variable $shutdown$ is used to identify whether cases were or were not exported from Wuhan on or after 23 January 2020.

The role of control measures at different stages of the outbreak are captured by estimated parameter C (range 0-1), which reduces transmission and R_0 proportionally as a multiplicand of β . The timing and implementation of transmission control measures in the 342 cities and 31 provinces are shown in Fig. S4. Before 22 January 2020, there were no recorded interventions thus $C_0=1$. From 23 January onwards, provinces gradually scaled up Level 1 emergency responses (stage 1), with effects measured as C_1 (Fig. S4). Because the effects of control measures varied among provinces during the scale-up, C_1 was grouped into high C_{1_high} , medium C_{1_medium} , and low

646 C_{I_low} . The allocation of provinces to groups was made by proposing several alternative
 647 hypotheses and testing each by model fitting (Table 3, Table S4). Stage 2 of control (C_2) began
 648 when more than 95% of cities in a province had implemented control measures, including the
 649 closure of entertainment venues, suspension of intra-city public transport or prohibition of travel
 650 by any means to and from other cities (see above). In Hubei Province (except Wuhan city), stage 2
 651 included the use of shelter or “Fang Cang” hospitals from early February onwards.
 652
 653 Model fitting was performed using the Metropolis–Hastings Markov chain Monte Carlo (MCMC)
 654 algorithm with the MATLAB (version R2016b) toolbox DRAM (Delayed Rejection Adaptive
 655 Metropolis). Prior estimates of the mean and (Gaussian) variance of R_0 , δ , and γ were derived from
 656 epidemiological surveys (27). There was no evidence to inform a prior for the reporting rate ρ , the
 657 proportion of cases that were reported among all latent and infectious individuals in Wuhan.
 658 Systematic surveys of infection (e.g. by serological testing) have not yet been reported. In the
 659 absence of any guiding data, ρ was given a prior uniform distribution between 0 and 1.
 660
 661 After a burn-in of 1 million iterations, we ran the MCMC simulation for a further 10 million
 662 iterations, sampled at every 1000th step to avoid auto-correlation. Trace plots and Gelman and
 663 Rubin diagnostics were used to judge convergence of the MCMC chains (Fig. S4). Each fitting
 664 exercise was repeated three times to test the robustness of results, which converged to the same
 665 estimates on each occasion (Fig. S5). We used the fitted SEIR model, with posterior estimates of
 666 parameter values, to simulate outbreaks outside Wuhan, with and without the Wuhan travel ban
 667 and with and without the national emergency response (Fig. 4B).
 668

669



670

671

672

673

674

675

676

677

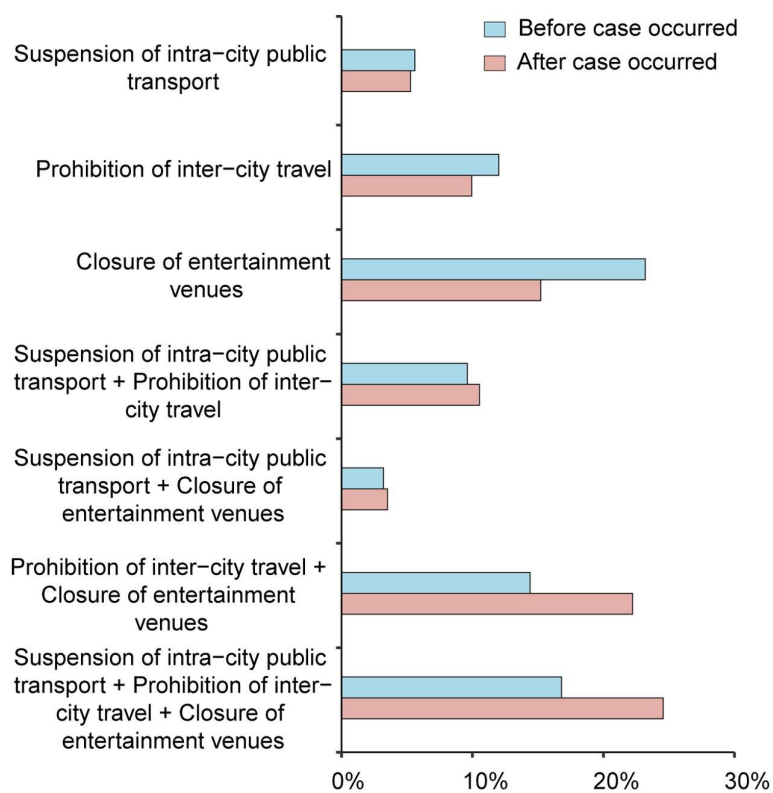
678

679

Fig. S1. Patterns of COVID-19 dispersal out of Wuhan (Hubei province) to other provinces by time and geographical distance. (A) Daily reports of confirmed cases from each of 31 provinces. Provinces are ranked by decreasing volume of people leaving Wuhan for other destinations, to elsewhere in Hubei Province (top) and to Tibet (bottom). (B) Synchrony of epidemics in different provinces in relation to distance between provinces. Synchrony is measured by the correlation between the number of cases reported in two provinces on each day, using a spatial non-parametric correlation function (28).

680

681



682

683 **Fig. S2.** Percentage of cities that implemented three kinds of transmission control measures before
 684 (blue), or on the same day or after (red), the first case was reported.

685

686

687

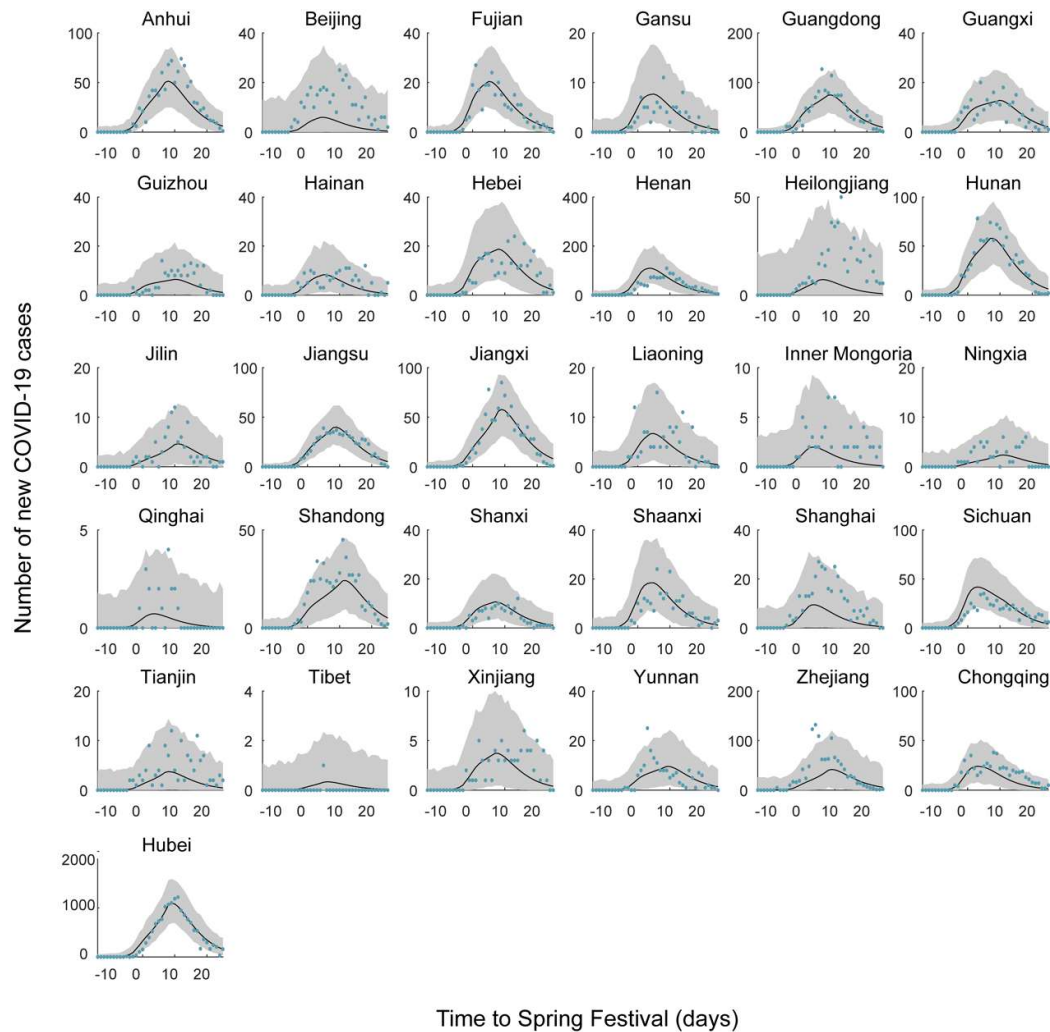
688

689

690

691

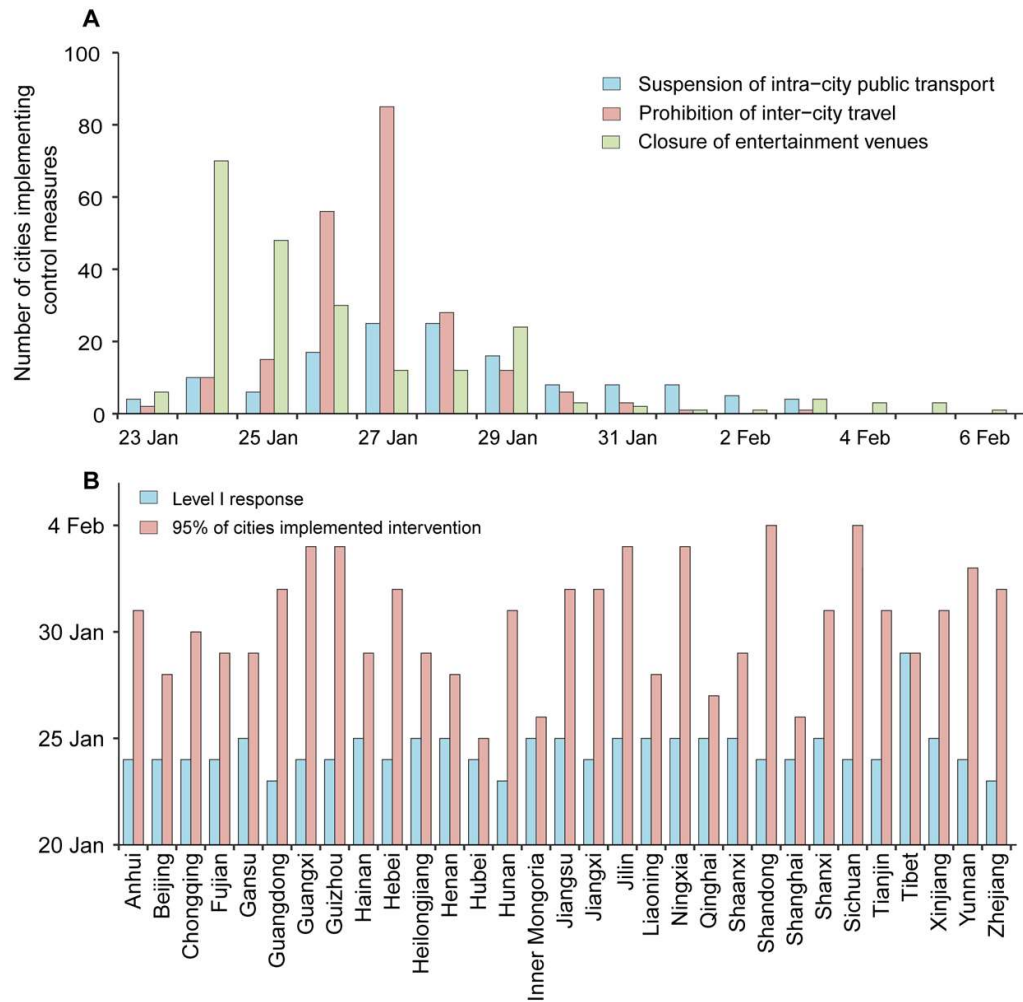
692
693



694
695
696
697
698
699
700
701
702
703
704

Fig. S3. Fits of the SEIR epidemic model to time series of reported cases from 31 provinces. The numbers of confirmed cases reported (points) and estimated (lines) each day in each provinces (Hubei excludes Wuhan city). Grey areas correspond to pointwise 95% prediction envelopes. The period covers the 40 days of the Spring Festival, from 15 days before to 25 days after the Chinese Lunar New Year. The Spring Festival travel ended on 19 February, day 50 of the epidemic.

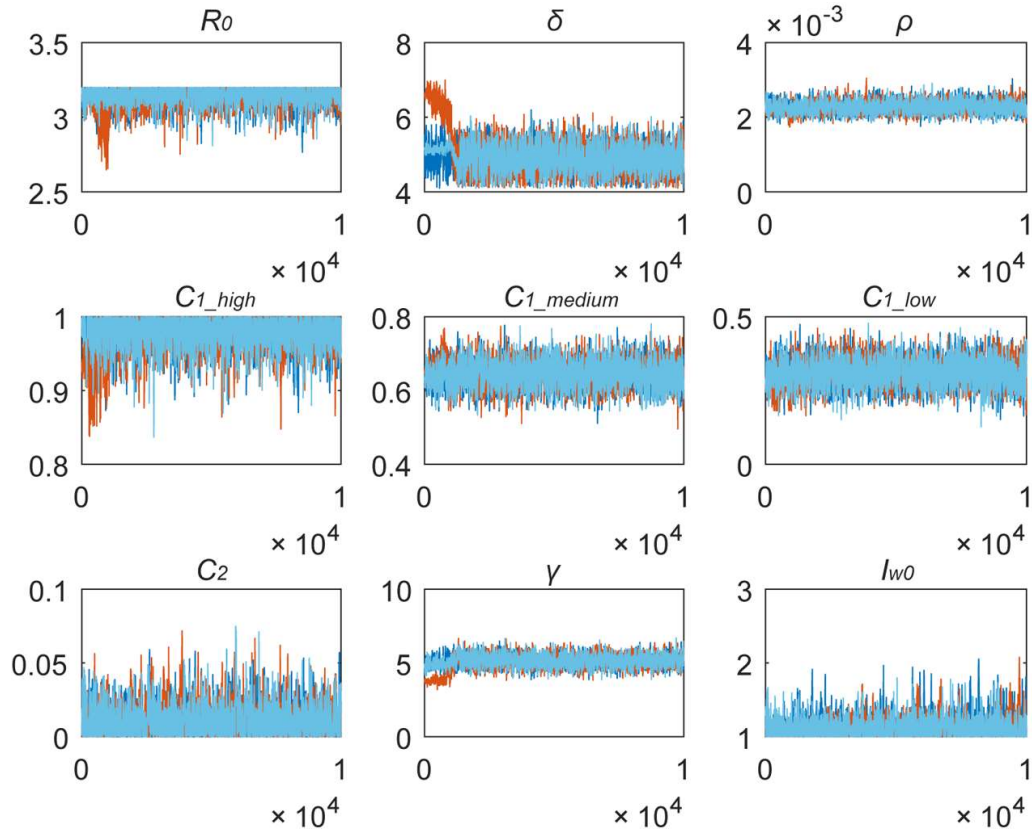
705
706



707
708
709
710
711
712
713
714

Fig. S4. (A) The number of cities implementing three interventions by date in 342 cities (see also Fig. S2). (B) Dates (vertical axis) on which the Level 1 emergency response began (blue, start of stage 1), and on which 95% of cities had implemented transmission control measures (red, end of stage 1, beginning of stage 2), in 31 provinces.

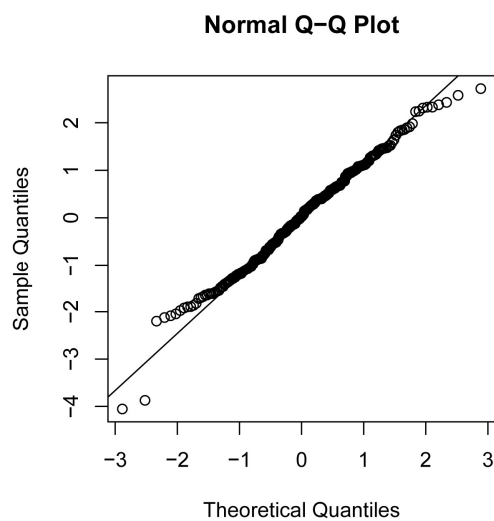
715
716



717
718
719
720
721
722
723

Fig. S5. Trace plots of parameter values for the epidemic model, estimated by Bayesian Markov Chain Monte Carlo (MCMC) methods. The three different colours represent three runs of the MCMC model, with one run (light blue) presented at the forefront.

724



725

726 **Fig. S6.** Q-Q plot the residuals of the linear regression analysis on the association between the
727 Wuhan travel ban and dispersion of COVID-19 across cities in China.

728

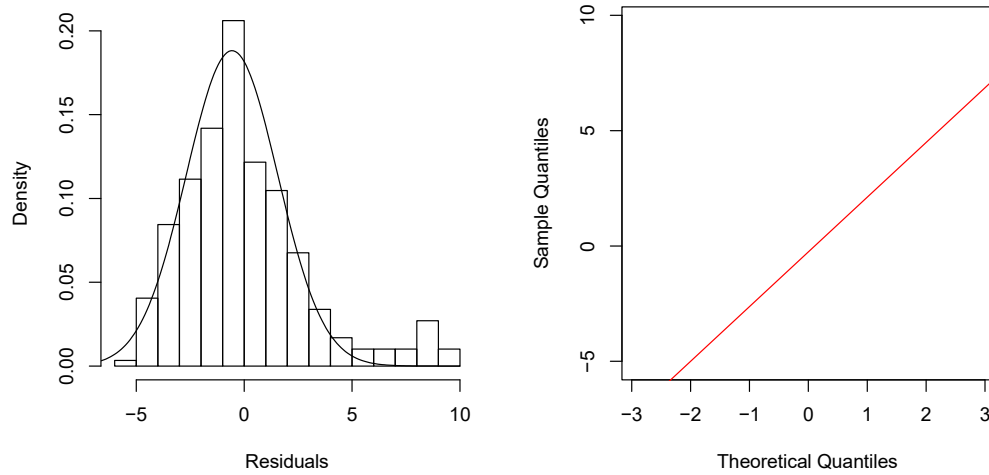


Fig. S7. Histogram and Q-Q plot the residuals of the log-linear regression analysis on the associations between the transmission control measures and incident per capita divided by inflow from Wuhan, across cities in China.

734

735

736 **Table S1.** Candidate statistical models used to study the association between the Wuhan city travel

737 ban and the arrival time of COVID-19 in other cities (see Table 1 of the main text). The chosen

738 model is shown in bold face.

739

Model	AIC*
Y=log10(TotalFlow) + log10(AirFlow) + log10(RoadFlow) + log10(TrainFlow) + log10(Pop) + log10(Dis) + Lat + Long + Shutdown	113.73
Y=log10(TotalFlow) + log10(AirFlow) + log10(RoadFlow) + log10(Pop) + log10(Dis) + Lat + Long + Shutdown	111.91
Y=log10(TotalFlow) + log10(AirFlow) + log10(Pop) + log10(Dis) + Lat + Long + Shutdown	110.63
Y=log10(TotalFlow) + log10(Pop) + log10(Dis) + Lat + Long + Shutdown	109.83
Y=log10(TotalFlow) + log10(Pop) + Lat + Long + Shutdown	108.57

740 * Akaike information criterion

741

742

743

744

745 **Table S2.** Summary of interventions and their timing across 342 cities (see Table 2 of the main
 746 text).

747

Level 1 response to major public health emergencies	Number of cities implementing control measures	Average lags (days) between implementation and 31 December 2019‡
Identify the affected area of a city*	342	0
Close schools*	342	0
Close entertainment venues and ban public gatherings	220	27.17 (2.82)
Isolate patients with infectious diseases*	342	0
Isolate suspected patients*	342	0
Suspend intra-city public transport (bus and subway)	136	29.00 (2.60)
Prohibit inter-city travel	219	27.86 (1.49)
Collect, evaluate, report and publish information on public health emergencies daily*	342	0
Assist subdistrict, township (town), neighbourhood and village committee staff*	342	25.32 (1.07)

748 *Interventions implemented immediately were not included in the regression analysis.

749 ‡Summary statistics reported for timing are mean (standard deviation).

750

751

752

Table S3. Associations of the type and timing of transmission control measures with the number of cases reported during the first week of outbreak in a new location (city), estimated from a log-linear regression model. This analysis checks and confirms the robustness of results in Table 2 of the main text. As described in the main text, the prohibition of inter-city travel, the third intervention that was investigated in this study, did not significantly reduce the number of cases reported during the first week of city outbreaks.

Least square estimates			
Covariates	Coefficient	95% CI	P
(Intercept)	-1.18	(-4.96, 2.61)	0.54
Arrival time	0.27	(0.12, 0.42)	<0.01
Suspension of intra-city public transport			
Implementation	-12.71	(-21.77, -3.64)	<0.01
Timing	0.46	(0.13, 0.80)	<0.01
Closure of entertainment venues			
Implementation	-3.41	(-5.73, -1.10)	<0.01
Timing (discretised)	1.51	(0.66, 2.36)	<0.01
Bootstrap estimates			
Covariates	Coefficient	95% CI	P
(Intercept)	-1.18	(-4.45, 2.14)	0.49
Arrival time	0.27	(0.14, 0.40)	<0.01
Suspension of intra-city public transport			
Implementation	-12.66	(-21.37, -4.74)	<0.01
Timing	0.46	(0.17, 0.80)	<0.01
Closure of entertainment venues			
Implementation	-3.42	(-5.82, -0.86)	<0.01
Timing (discretised)	1.51	(0.57, 2.44)	<0.01

763

764

765 **Table S4.** Candidate models used to characterize the association between control measures and the
 766 new confirmed cases reported each day in different provinces (see Table 3 of the main text). Based
 767 on the deviance information criterion (DIC), the chosen model is shown in bold face.

768

Model	DIC* (mean) ‡	DIC (median)
Universal C , γ	117.55	38.97
Universal $C1$, $C2$, γ	78.81	28.41
$C1_high$, $C1_medium$, $C1_low$, $C2$, γ	55.66	27.43
$C1_high$, $C1_low$, $C2$, γ	62.31	28.13
$C1_high$, $C1_medium$, $C1_low$, γ	110.95	34.76

769

* Distribution for provinces

770

‡ The deviance information criterion

771

$C1_high$, Effect of control in stage 1, high

772

$C1_medium$, Effect of control in stage 1, medium

773

$C1_low$, Effect of control in stage 1, low

774

$C2$, Effect of control in stage 2

775

γ , Rate of removal of infectious cases before isolation

776

High, medium and low represent the efficacy of control measures in three groups of provinces.

777

778

References

19. J. T. Wu, K. Leung, G. M. Leung, Nowcasting and forecasting the potential domestic and international spread of the 2019-nCoV outbreak originating in Wuhan, China: a modelling study. *Lancet* 395, 689-697 (2020).
20. B. Ripley, B. Venables, D. M. Bates, K. Hornik, A. Gebhardt, D. Firth, M. B. Ripley, Package 'MASS'. CRAN Repository, See <http://cran.r-project.org/web/packages/MASS/MASS.pdf> (2013).
21. B. R. Kirkwood, J. A. Sterne, Essential medical statistics. (John Wiley & Sons, 2010).
22. D. E. Bailey, Probability and Statistics. (John Wiley & Sons, 1971).
23. A. Canty, B. Ripley, boot: Bootstrap R (S-Plus) functions. R package version 1.3-24. (2019).
24. A. C. Davison, D. V. Hinkley, Bootstrap methods and their application. (Cambridge university press, Cambridge, 1997).
25. R. M. Anderson, R. M. May, Infectious Diseases of Humans: Dynamics and Control. (Oxford Univ Press, Oxford, 1992).
26. A. Morton, B. F. Finkenstädt, Discrete time modelling of disease incidence time series by using Markov chain Monte Carlo methods. *J R Stat Soc C* 54, 575-594 (2005).
27. Q. Li, X. Guan, P. Wu, X. Wang, L. Zhou, Y. Tong, R. Ren, K. S. M. Leung, E. H. Y. Lau, J. Y. Wong, X. Xing, N. Xiang, Y. Wu, C. Li, Q. Chen, D. Li, T. Liu, J. Zhao, M. Li, W. Tu, C. Chen, L. Jin, R. Yang, Q. Wang, S. Zhou, R. Wang, H. Liu, Y. Luo, Y. Liu, G. Shao, H. Li, Z. Tao, Y. Yang, Z. Deng, B. Liu, Z. Ma, Y. Zhang, G. Shi, T. T. Y. Lam, J. T. K. Wu, G. F. Gao, B. J. Cowling, B. Yang, G. M. Leung, Z. Feng, Early transmission dynamics in Wuhan, China, of novel coronavirus-infected pneumonia. *N Engl J Med* 382, 1199-1207 (2020)10.1056/NEJMoa2001316).
28. O. N. Bjørnstad, R. A. Ims, X. Lambin, Spatial population dynamics: analyzing patterns and processes of population synchrony. *Trends Ecol Evol* 14, 427-432 (1999).